# Synthesis optimization and charge carrier transfer mechanism in $LiLuSiO_4$:Ce, Tm storage phosphor

Dobrowolska, Anna; Bos, Adrie J.J.; Dorenbos, Pieter

**DOI**
10.1016/j.radmeas.2019.106147

**Publication date**
2019

**Document Version**
Accepted author manuscript

**Published in**
Radiation Measurements

# Synthesis optimization and charge carrier transfer mechanism in $LiLuSiO_4$:Ce,Tm storage phosphor

Anna Dobrowolska *, Adrie J.J. Bos, Pieter Dorenbos

*Delft University of Technology, Faculty of Applied Sciences, Department of Radiation Science and Technology, section Luminescence Materials*

*Mekelweg 15, 2629JB Delft, The Netherlands*

**Abstract**

$LiLuSiO_4$:Ce and $LiLuSiO_4$:Ce,Tm show very efficient charge carrier storage properties upon beta irradiation after samples have received treatment in vacuum. They outperform the commercial storage phosphor BaFBr(I):$Eu^{2+}$ in many aspects. The influence of the synthesis conditions, Ce and Tm concentration, nonstoichiometry and codoping with Ca, Hf, Al and Ge are reported. Based on the results of the synthesis optimization, thermoluminescence (TL) emission and TL excitation spectra a mechanism of charge carrier transfer, storage, and recombination during irradiation and thermal or optical readout is proposed.

**Keywords**: thermoluminescence, storage phosphors, cerium, thulium, charge transfer

## 1. Introduction

We recently discovered that $LiLuSiO_4$:Ce and $LiLuSiO_4$:Ce,Tm are very efficient storage phosphors after they have received treatment in reducing atmosphere [1]. After a heat treatment in $H_2N_2$ storage capacity increases 10-fold, and is then already 2 times better storing than BaFBr(I):Eu. Again 2-3 times better storage capacity is obtained after a heat

* Corresponding author. E-mail address: apdobrowolska@wp.pl (Anna Dobrowolska)

treatment in vacuum. The best sample, $LiLuSiO_4$:Ce,Tm has over four times higher storage capacity than the state-of-the-art storage phosphor BaFBr(I):Eu and it does not show fading of stored information with time. It is not hygroscopic and has higher density (5.61 g $cm^{-3}$) than today's commercial phosphor BaFBr(I) (5 g $cm^{-3}$ [2]). Trapped charge carriers produced during irradiation can be efficiently liberated by a 475 nm blue LED and to lesser extent by a red laser. With such characteristics $LiLuSiO_4$:Ce,Tm is in many aspects a better alternative for BaFBr(I):Eu.

The performance of optimized $LiLuSiO_4$:Ce;Tm as a storage phosphor was evaluated in [1]. Here, we studied how the preparation method and co-doping influences thermoluminescence (TL), TL emission and TL excitation spectra. The results provide an understanding of the nature of the traps, and the charging and recombination mechanism.

## 2. Materials and Methods

$LiLuSiO_4$, $LiLu_{1-x}Ce_xSiO_4$, $LiLu_{1-x}Tm_xSiO_4$, $LiLu_{(1-3x)}Ce_xTm_xM_xSiO_4$, where M= Hf, Ca, Ge, $LiLu_{(1-2x)}Ce_xTm_xSi_{1-y}Al_yO_4$, samples with x ranging from 0.0005-0.1 and y = 0.05, were prepared with the solid state method. The starting materials were lithium carbonate ($Li_2CO_3$, 99.999 %, Alfa Aesar), lutetium oxide ($Lu_2O_3$, 99.999 %), cerium oxide ($CeO_2$; 99.99 %), thulium oxide ($Tm_2O_3$; 99.99%), silicon oxide ($SiO_2$, 99.99 %), hafnium oxide ($HfO_2$, 99.99%), aluminium oxide ($Al_2O_3$, 99.95%), germanium oxide ($GeO_2$, 99.999%), calcium carbonate ($CaCO_3$, 99.99%). All starting materials were thoroughly grinded with acetone as a wetting medium and heated at 800 $^oC$ for 8-10 h in air and reheated after regrinding at 1150 $^oC$ for 15 h in air. Then, some samples were reheated once at 1150 $^oC$ or twice for 5 hrs in reducing conditions of $H_2$(7%)-$N_2$ or in vacuum. Samples heated only in air or only in vacuum have a white body colour. After annealing in $H_2$(7%)-$N_2$ samples become slightly grayish. The crystal purity of the synthesized samples was checked by comparing the XRD patterns with that of isostructural $LiYbSiO_4$ PDF#00-048-0013 (Pearson's Crystal Structure Database, 2014/15) as well as with the pattern for $LiLuSiO_4$ published elsewhere [3]. All produced materials were of single phase.

Thermoluminescence measurements were performed with a RISØ TL/OSL reader model DA-15 and a controller model DA-20. The emission observed during the thermoluminescence experiments was detected with a 2 mm Schott BG39 filter placed in

front of an EMI 9635QA photomultiplier tube (PMT). It provides a detection window between 320 and 650 nm, suitable for selecting the $Ce^{3+}$ emission of the investigated samples. Samples were irradiated with a $^{90}Sr/^{90}Y$ beta source with a dose rate of 0.7 mGy $s^{-1}$. All measurements were executed under a flow of nitrogen gas. Powder samples with masses < 20 mg and area ~ 0.5 $cm^2$ were investigated.

The optical stimulations were performed with either a blue LED or a red laser. The blue LED with $\lambda_{max.}$ = 475 nm and about 8 mW $cm^{-2}$ power is within the RISO reader. A U340 7.5 mm filter with a transmission between 270-380 nm was employed during stimulation. Note that only a small fraction of light emitted by the phosphor ($Ce^{3+}$ emission 350-550 nm) is then detected. The TL after stimulation with a red laser with $\lambda_{exc.}$ = 635 nm and about 2 mW $cm^{-2}$ power was measured with a BG39 2 mm filter transmitting well the $Ce^{3+}$ emission. Additionally, a shutter and lens were installed between the sample and PMT. The shutter prevents over exposure of the PMT during stimulation and the lens increases the light collection efficiency.

The TL emission spectrum (TLEM) was measured using an Ocean Optics, QE65000 UV-VIS spectrometer with a HR composite grating (300 lines $mm^{-1}$) and an entrance aperture of 100 μm resulting in a 3.3 nm (FWHM) wavelength resolution in the 200 to 900 nm spectral range. Samples were irradiated with a $^{60}Co$ gamma source to an absorbed dose of 2 kGy.

## 3. Results

### 3.1. Photoluminescence

Figure 1 presents photoluminescence emission and excitation spectra of undoped (a) and Ce-doped $LiLuSiO_4$ (b). The luminescence of undoped $LiLuSiO_4$ is composed of several overlapping bands between 5 and 2 eV. The excitation spectra were measured for emission energies of 3.01, 4.28 and 3.58 eV. They consist of bands at 8.41, 7.28, 6.65 eV; 7.17, 6.26 eV and 8.41, 7.28, 5.45 eV, respectively. The emission spectrum of $LiLuSiO_4$:Ce(0.1%) is dominated by a band at 3.03 eV (410 nm). The excitation spectrum of $Ce^{3+}$ contains a series of bands at 7.29, 4.92, 4.13 (shoulder), 3.93 and 3.52 eV. Samples doped with Ce

and co-doped with Tm, Hf, Nb, Ge, Ca, Gd and Al show the same emission and excitation characteristics as the one doped only with Ce. Ge co-doping noticeably increases the intensity of host related excitation bands and apparently Ge doping increases the transfer efficiency from the host to $Ce^{3+}$ (data not presented here).

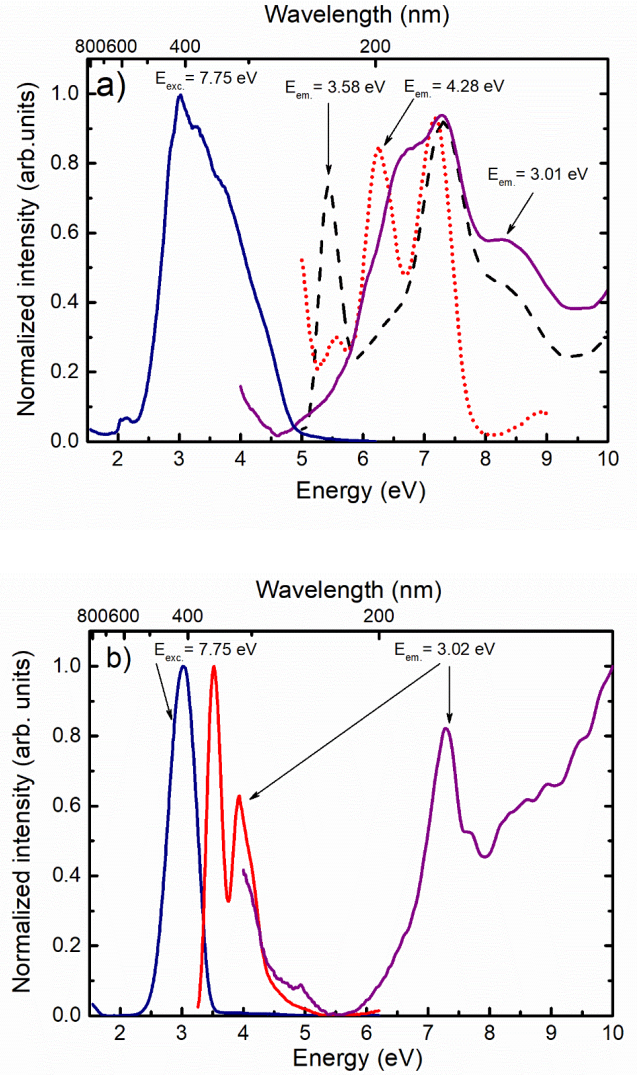


**Figure 1.** Photoluminescence emission and excitation spectra recorded at 20 $^{o}$C of undoped (a) and Ce-doped $LiLuSiO_4$ (b). Excitation and emission energies are indicated with the spectra.

### 3.2.Thermoluminescence studies

The thermoluminescence yield (TY) and fading properties were used as a measure of the storage capacity of the samples. Thermoluminescence yield is defined as the integrated TL glow peak area corrected for sample mass (mg) and β particle irradiation time (s). All measurements were performed with the same heating rate (β=5 $^{o}$C $s^{-1}$), filter (BG39 2mm) and PMT (EMI 9635QA). The emission observed during TL readout was always in the same spectral range. Fading is a loss of trapped charges with time. The integrated area of the TL glow peak as a function of the time elapsed after irradiation provides the so-called fading rate curves.

Figure 2 presents the thermoluminescence glow curves of undoped, Ce-doped, Tm-doped and Ce,Tm doped samples synthesized in air and then reheated in vacuum. Glow curves of undoped and Tm-doped only samples are composed of glow peaks with maxima at around 60, 160 and 230 $^{o}$C when measured with β = 5 $^{o}$C $s^{-1}$, hereafter referred to as glow peak 1+2, 4, and 5 respectively. The glow curve of the Ce-doped sample in Fig. 2c consists of the glow peaks 1+2, 5 plus an additional one at around 110 $^{o}$C hereafter referred to as peak 3. In the sample doped with Ce and Tm, the TL in Fig. 2d is dominated by glow peak 5. Both samples containing Ce show two orders of magnitude higher thermoluminescence intensity.

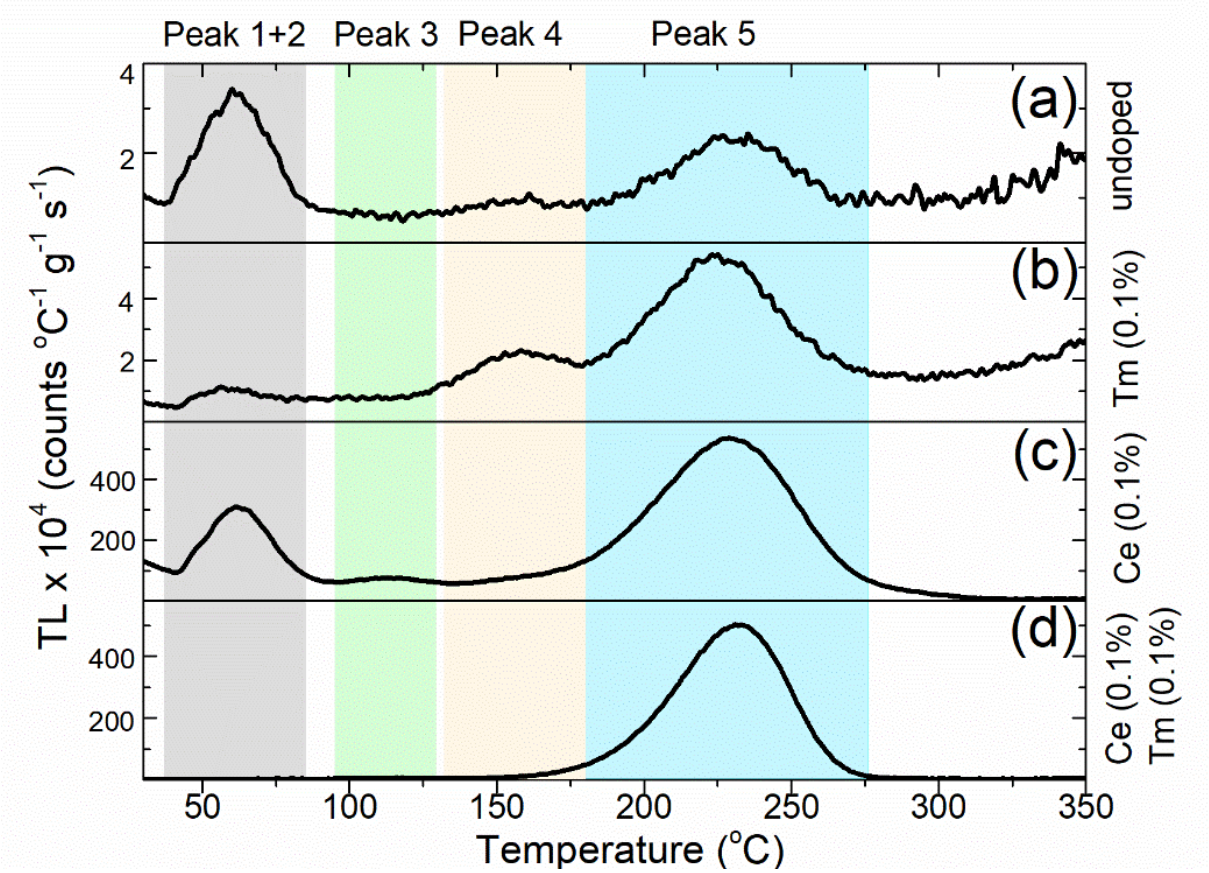


**Figure 2.** TL glow curves for $LiLuSiO_4$ undoped (a), Tm(0.1%)-doped (b), Ce(0.1%)-doped (c) and Ce(0.1%),Tm(0.1%)-doped (d) measured with $\beta = 5\ ^{o}C\ s^{-1}$. Note that the intensity scales in a) and b) are smaller by a factor of 100 than for c) and d).

The thermoluminescence glow curves were measured after various doses of irradiation. The position of the glow peaks does not shift with the dose which indicates first order recombination kinetics [4] with negligible re-trapping of charge carriers. The trap depth of peak 5 was determined using the variable heating rate method resulting in a trap depth E = 1.44 eV and a frequency factor $s = 3.2\ 10^{13}\ s^{-1}$ (see supplementary data). The other glow peaks turn out not to be so relevant for the storage properties of our best sample of $LiLuSiO_4$:Ce;Tm and will not be further analyzed.

Figure 3 presents contour plots of TL emission spectra for $LiLuSiO_4$ undoped (a), Tm (0.1%) (b), Ce (0.1%) (c) and Ce (0.1%), Tm (0.1%) (d). The horizontal axis shows the emission wavelength and the vertical axis the TL temperature. All spectra were recorded

under similar experimental conditions. At the top of Fig. 3a the emission spectra at the temperature of peak 2 and of peak 5 are projected. The spectrum measured at peak 2 contains two broad emission bands at 370 nm (strong) and 600 nm (weak). The spectrum measured at peak 5 contains line emissions at 377 nm, 413 nm, 435 nm, and 458 nm related to $^5D_3$-$^7F_J$ transitions and at 550 nm and 609 nm related to $^5D_4$-$^7F_J$ (545-625 nm) transitions in $Tb^{3+}$ that are superimposed on broad emission bands peaking around 400 nm (weak) and 600 nm (strong). Contamination with $Tb^{3+}$ originates from the starting materials and it was also found by us in [5, 6]. The emission spectrum recorded at peak 5 has an additional band at around 700 nm. At the right axis of the contour plot the thermoluminescence glow curves recorded at 379 nm, where the $Tb^{3+}$ line emission is superposed on a broad emission, and at 594 nm broad band emission are projected. Emissions at 379 nm and 594 nm appear when the traps responsible for the glow peaks 2, 4, 5 and 2, 4 and a new peak 6 at 292 ºC are emptied, respectively. Fig. 3b presents TL emission for $LiLuSiO_4$:Tm (0.1%) which is very similar to that of the undoped sample. There are only differences in the intensity of the observed emissions and TL glow peaks.

TL emission of $LiLuSiO_4$:Ce (0.1%) in Fig. 3c shows that Ce is the only recombination centre. TL emission of the Ce,Tm codoped sample shows also only $Ce^{3+}$ emission and glow peak 5 is even more dominating. All glow peaks observed in undoped samples are also present in Ce-, Tm- and Ce,Tm- doped samples but with different intensity. In the Ce-doped samples glow peak 5 in Fig. 3c,d is like in Fig. 2c and 2d 50 to 100 times more intense than for the undoped or Tm only doped sample.

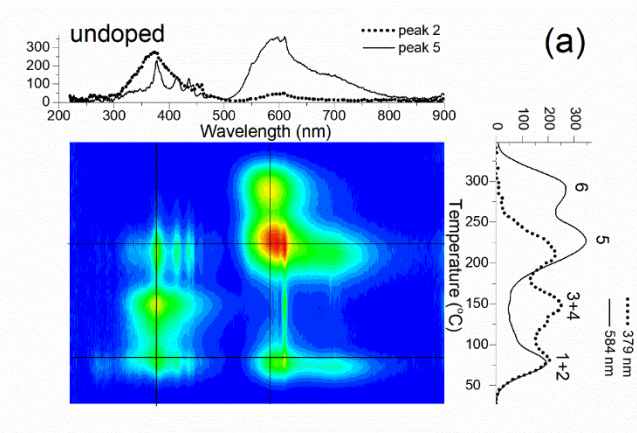

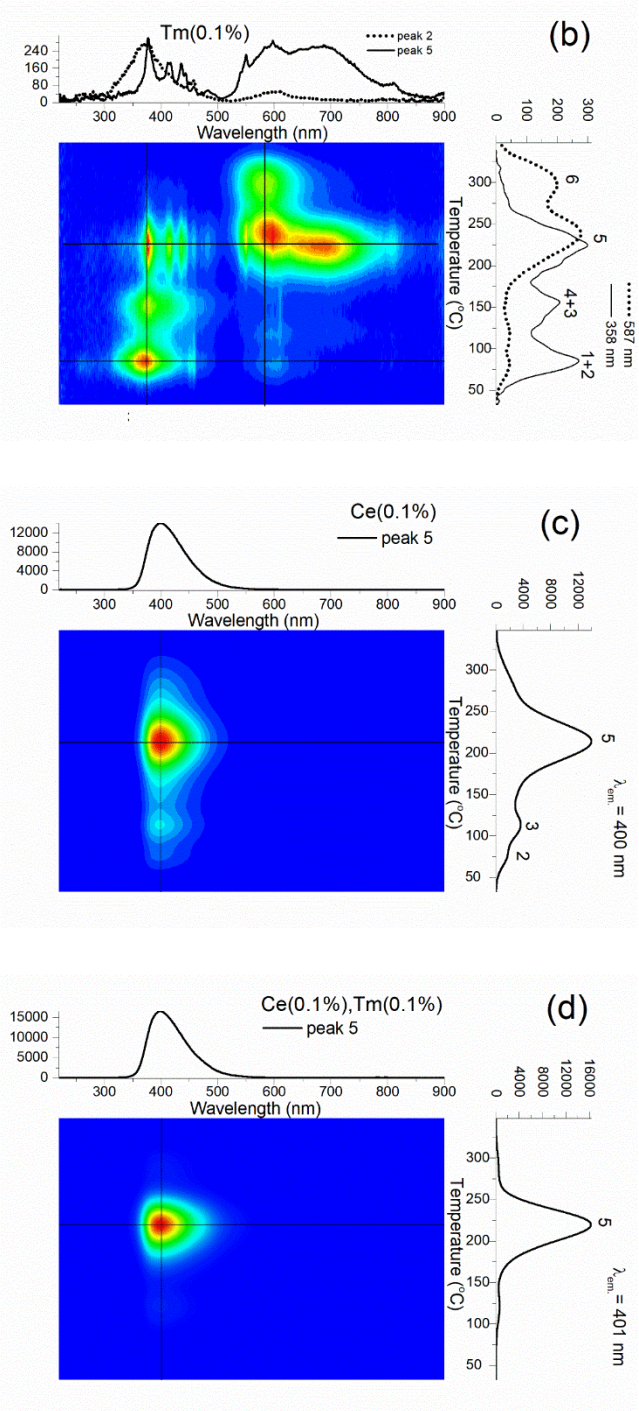


**Figure 3.** TL emission spectra of $LiLuSiO_4$ undoped (a), doped with 0.1% Tm (b), doped with 0.1% Ce (c), and doubly doped with 0.1% Ce and 0.1% Tm (d).

Fig. 4a presents the TL glow curves after beta irradiation of $LiLuSiO_4$:Ce (0.5%), Tm (0.5%) as synthesized in air, reheated once in $H_2N_2$, reheated twice in $H_2N_2$,or reheated once in vacuum. The heating in reducing atmosphere was meant to increase the thermoluminescence intensity. In all cases TL is dominated by glow peak 5. The thermoluminescence yield TY increases by a factor of more than 50 from a value of 4 for the sample synthesized in air to 71 and 107 for the samples heated in $H_2N_2$ once and twice, and to 215 for the sample heated in vacuum. The second heating in $H_2N_2$ leads to significant broadening of the glow peak.

Fading rate curves are shown in Fig. 4b. The sample prepared in air, which shows the lowest TY = 4 in Fig. 4a, shows the fastest fading. The TL intensity drops to 47 % of the initial value after 4 hours of storage at room temperature in darkness. Samples heated in $H_2N_2$ or heated in vacuum show much less fading after 4 hours. The intensity drops to 87 % for the sample heated once in $H_2N_2$ and to 92 % for the sample heated twice in $H_2N_2$, and curve 4) for the sample heated in vacuum runs in between.

The TL glow curves of $LiLuSiO_4$: Ce(0.1%), Tm(0.1%) synthesized in air, then heated in vacuum and reheated in air were measured (Supplementary Information). The sample heated only in air shows relatively weak thermoluminescence (TY = 27). Heating in vacuum increases the overall TL intensity with a factor of ten (TY = 261). Reheating of the sample in air that were treated before in vacuum lowers again significantly the TL intensity (TY = 47). This all implies that the effect of the thermal treatment is reversible.

In order to study the charging of the phosphor, TL recordings were performed after laser light or Xe-lamp light excitation instead of β-irradiation. Figure 5 shows thermoluminescence glow curves of the 0.5% Ce and 0.5%Tm doped sample that was fired in air and subsequently in vacuum, and measured after 1800 s irradiation with the 475 nm (2.61 eV) blue LED at 25 $^oC$ (a) and at 50 $^oC$ (b). The former glow curve is dominated by the glow peak 6 at 310 $^oC$, the same glow observed in Fig. 3a and 3b provides broad band emission around 590 nm, which would be blocked by a filter in the experiment with blue diode. The latter glow curve is more complex and contains also glow peaks 4 and 5.

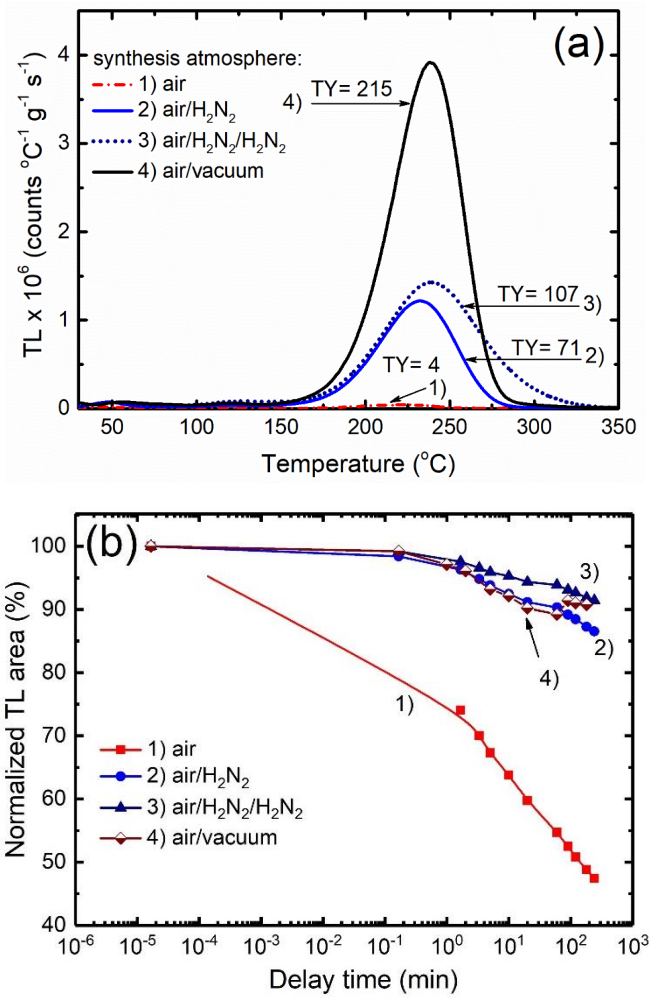


**Figure 4.** a) Thermoluminescence glow curves of $LiLuSiO_4$:Ce(0.5%),Tm(0.5%) synthesized 1) in air, 2) reheated in $H_2N_2$ once, 3) twice, or 4) in vacuum b) the corresponding fading rate curves.

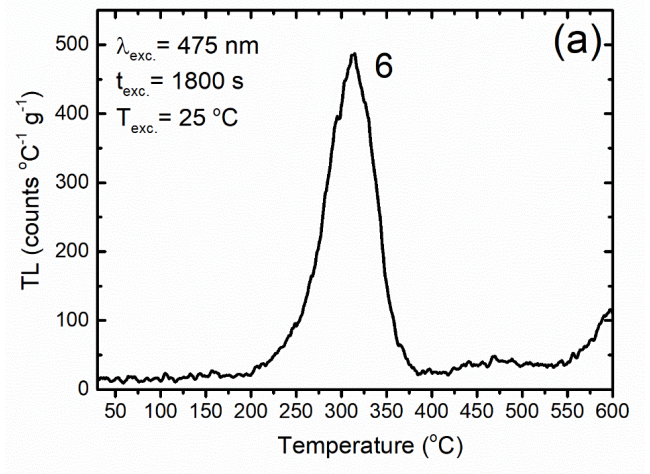

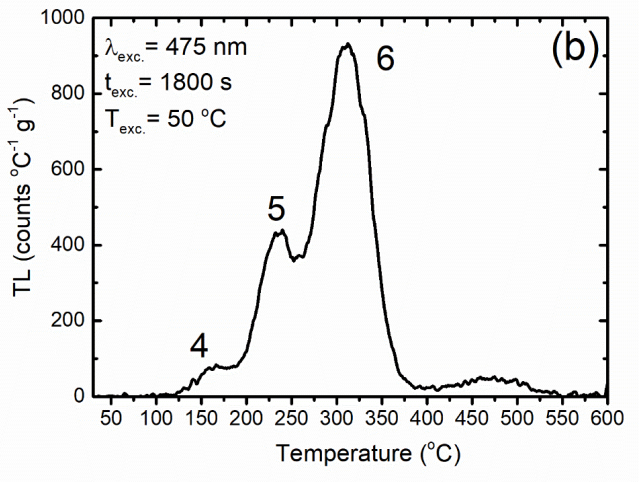


**Figure 5.** TL glow curves of $LiLuSiO_4$:Ce (0.5%), Tm (0.5%), recorded after excitation with 475 nm blue LED at $T_{exc}$ of 25 ºC (a) and 50 ºC (b) with $\beta$= 5 ºC $s^{-1}$.

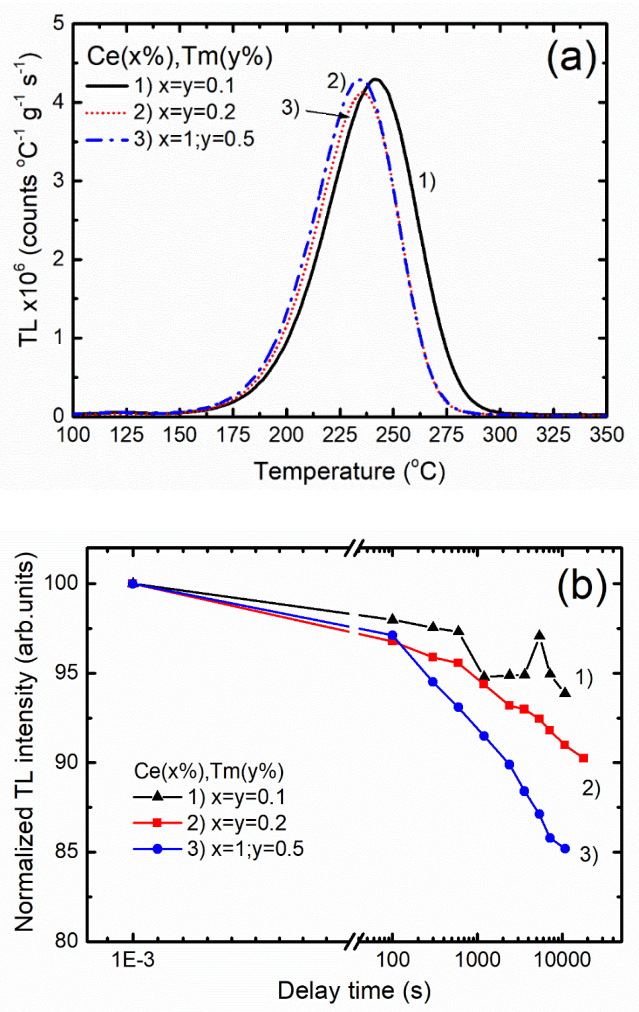

**Figure 6.** a) Thermoluminescence of $LiLuSiO_4$:x%Ce;y%Tm with various concentrations x and y, and b) the corresponding fading rate curves.

Fig. 6a displays the TL glow curves of $LiLuSiO_4$ with various concentration of Ce and Tm. All glow curves contain only glow peak 5 with a slightly different temperature at the peak maximum, but with very similar intensity. The sample with the lowest concentration of x = 0.1 % Ce and y = 0.1 % Tm has the highest value for peak temperature $T_m$. The fading rate curves presented in Fig. 6b indicate that fading of stored information increases with higher concentration.

Thermoluminescence excitation spectra (TLES) were measured to reveal the trap filling mechanism. Monochromatic light from a Xe-lamp in the range of 200-400 nm was used to excite charge carriers from defect levels to host band states that then populate charge carrier traps. Fig. 7 presents the TL glow curves and thermoluminescence excitation spectra for $LiLuSiO_4$: Ce (x%), Tm (x%), x = 0.1 (a, b); x = 0.2 (c, d); x = 0.5 (e, f). Fig.7a compares the TLES with the photoluminescence excitation spectrum (PLES) of $Ce^{3+}$ emission where the first three 4f-5d excitation bands can be seen as a shoulder band at 300 nm ($5d_3$), and as distinct peaks at 315 nm ($5d_2$), and 352 nm ($5d_1$). All TL glow curves in Fig. 7 are composed of the same glow peaks 1, 2, and 5 as defined in Fig. 2. The shape of the TLES does not depend on the Ce, Tm concentration. TLES spectra of glow peak 1 and 5 are composed of a weak band located at 359 nm corresponding with the lowest energy 4f-5d excitation band of $Ce^{3+}$ and an intense band at 280 nm that seems not related to Ce 4f-5d transitions. The TLES spectrum of glow peak 2 again consists of the excitation band at 359 nm but now it is much more intense, and there is another band at 290 nm with a weak shoulder band at 265 nm. The influence of the atmosphere on the trap filling mechanism was also investigated. The samples with 0.5% Tm and 0.5% Ce heated in vacuum were compared with the one heated in $H_2N_2$ (data not presented). There were no differences in the TLES indicating that the atmosphere during synthesis does not have significant influence on the trap filling mechanism.

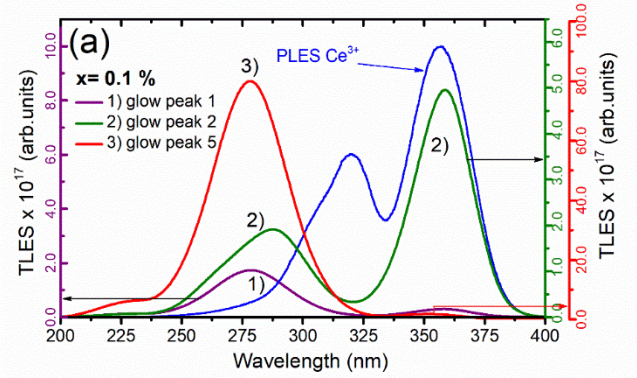
(a)
x= 0.1 %
1) glow peak 1
2) glow peak 2
3) glow peak 5
PLES Ce3+
3)
2)
1)
TLES x 10^17 (arb.units)
TLES x 10^17 (arb.units)
Wavelength (nm)

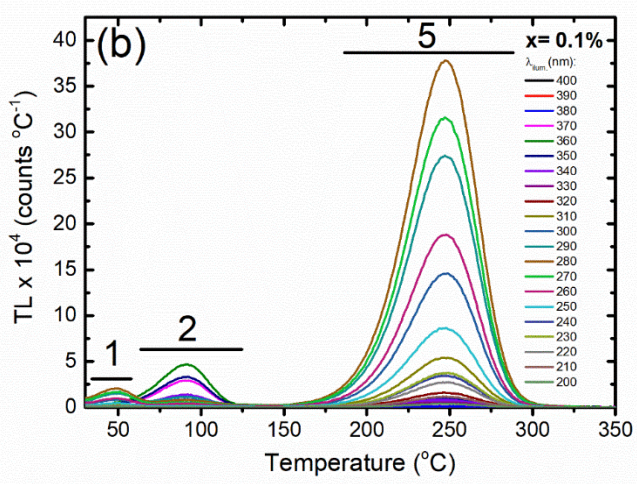
(b)
5
x= 0.1%
λ ium. (nm):
400
390
380
370
360
350
340
330
320
310
300
290
280
270
260
250
240
230
220
210
200
1
2
TL x 10^4 (counts °C^-1)
Temperature (°C)

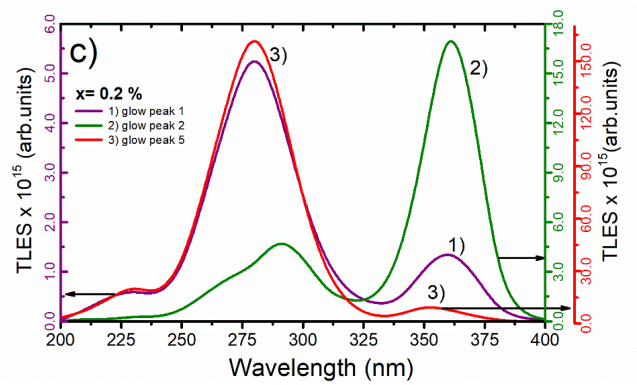
c)
x= 0.2 %
1) glow peak 1
2) glow peak 2
3) glow peak 5
3)
2)
1)
3)
TLES x 10^15 (arb.units)
TLES x 10^15(arb.units)
Wavelength (nm)

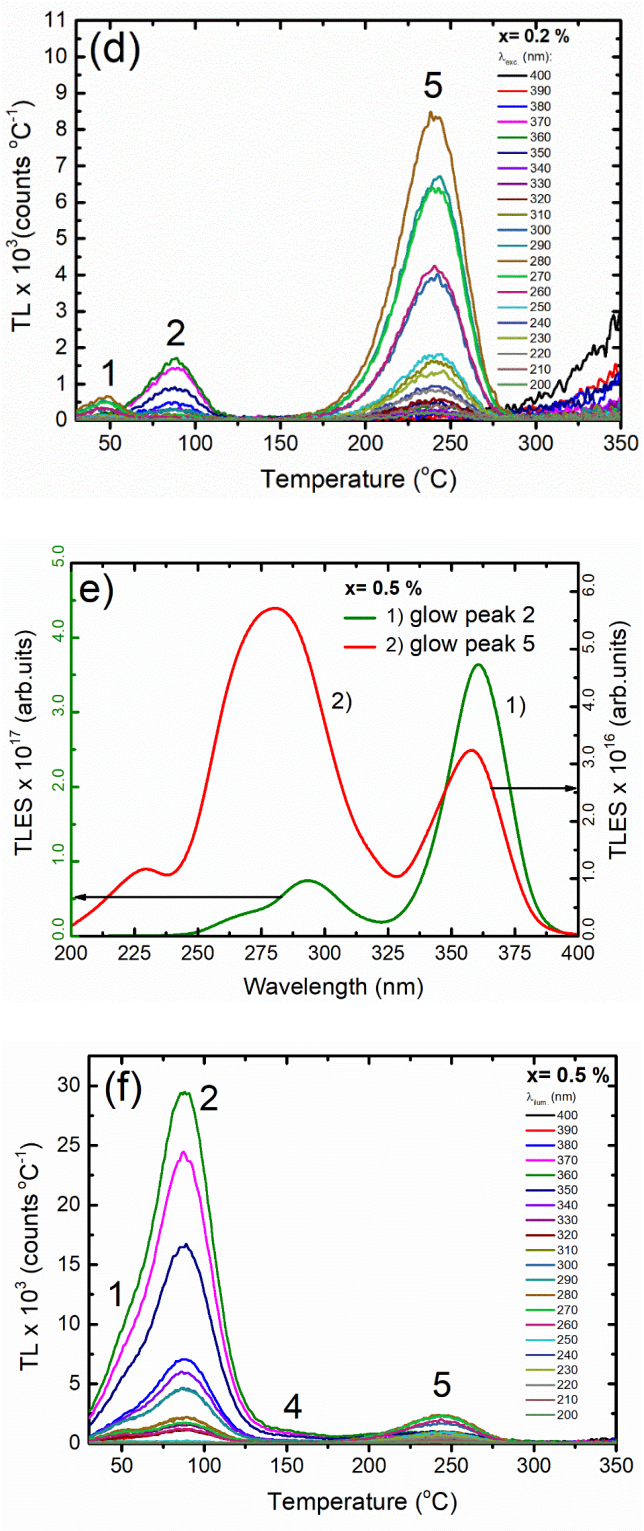


**Figure 7.** TL glow curves and thermoluminescence excitation spectra for $LiLuSiO_4$:Ce(x%),Tm(x%), x = 0.1 (a, b); x = 0.2 (c, d); x = 0.5 (e, f).

## 4. Discussion

To discuss the mechanism of charge carrier storage in $LiLuSiO_4$ and the role of the different dopants and defects therein it is very helpful to use the vacuum referred binding energy diagram with all divalent and trivalent lanthanide level energies as shown in Fig. 8. For diagram construction, the lanthanide parameters from [7] were used. The energy of 5.61 eV for the VB to $Eu^{3+}$ electron transition is from [6]. The energy for host exciton creation at about 10 K was estimated by adding 0.15 eV to the 7.3 eV energy observed in Fig. 1a at room temperature. A U-value of 6.90 eV from [8] was used.

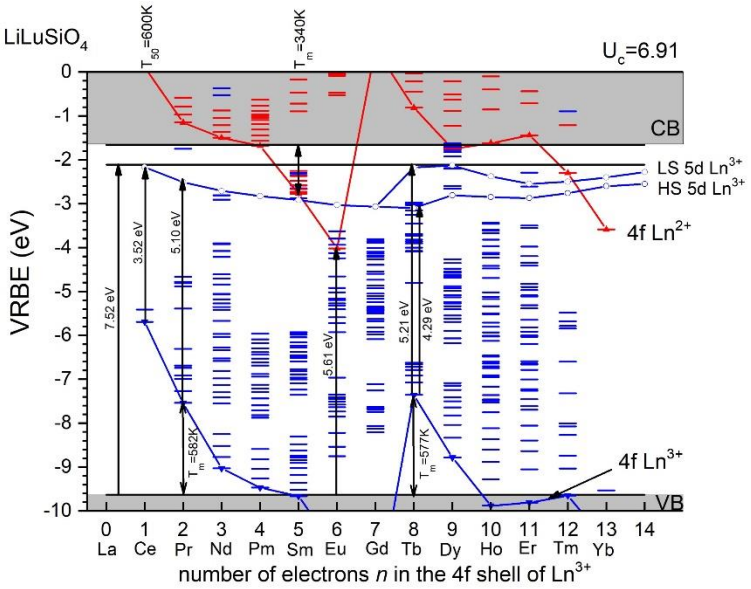


**Figure 8.** The vacuum referred binding energy diagram for $LiLuSiO_4$.

The luminescence characterization was performed for undoped; Ce- doped (see Fig. 1b); Ce, Tm-doped; and Ce, Tm, M = Ca, Ge, Hf, Al - doped samples (data not presented here). The luminescent features seen in the spectrum of the undoped sample in Fig. 1a are attributed to intrinsic host defects of unknown origin. The codopants Tm or M do not change the photoluminescence properties as compared to the sample doped only with Ce. The excitation peak around 7.30 eV is common to all excitation spectra and is attributed to the host exciton formation. The relatively high excitation intensity above 7.75 eV indicates that the host excitons efficiently transfers excitation energy to the defects giving emissions at 3.01 (412 nm) and 3.58 eV (346 nm). It is not excluded that the band to band excitation

lead not only to exciton formation but also to direct recombination of electrons and holes on the nearby defects. The host does not transfer energy to the defect producing emission at 4.28 eV (290 nm) as evidenced by the dotted curve in Fig. 1a.

Bands located at 3.52 eV (352 nm), 3.93 eV (316 nm), and 4.13 eV (300 nm) seen in the excitation spectrum of $Ce^{3+}$ emission in Fig. 1a are due to the 4f-$5d_{1,2,3}$ excitation of $Ce^{3+}$ in agreement with other reports [5, 6]. The 4f-$5d_{4,5}$ excitations of $Ce^{3+}$ that were observed as weak bands at 203 nm (6.11 eV) and 182 nm (6.81 eV) in [7] are not observed in Figure 1a. According to the VRBE diagram those two levels are well inside the conduction band, and their absence is most likely caused by a rapid delocalization and subsequent trapping thus preventing the radiative return to the ground state of $Ce^{3+}$.

Glow curves of undoped, Tm only, Ce only, and Ce,Tm codoped samples were measured to identify the trapping centres. All glow curves even that for the undoped sample in Fig. 2 are composed of the same glow peaks but with different intensity which suggests that all TL active traps have an intrinsic nature. Earlier studies [5, 6] on $LiLuSiO_4$:Ce;Sm revealed a glow curve near $T_m$ = 340 K that was attributed to the release of an electron from $Sm^{2+}$. The glow peak temperature is in accordance with the $Sm^{2+}$ ground state location below the conduction band bottom as in Fig. 8. Because $Tm^{3+}$ provides a 0.7 eV less deep electron trap than $Sm^{3+}$ its glow peak is expected below RT. With such intrinsic nature, the concentration of traps is expected to change upon synthesis conditions but not so much with dopant concentration which indeed appears so in Fig. 6a. The TL of the $LiLuSiO_4$:Ce (0.1%), Tm (0.1%) sample is very low after air-treatment (TY = 27), it increases tenfold upon heating in vacuum (TY = 261) and drops again upon reheating in air (TY = 47). This suggests that the traps are most likely related to oxygen vacancies created efficiently upon vacuum-treatment and removed again upon air-treatment [9].

TL emission spectra were measured to identify the recombination centres. Spectra for undoped and only Tm-doped samples in Figs. 3a,b are very similar, and the broad emission bands at around 400 and 600 nm are assigned to intrinsic host defect emissions, A broad band around 400 nm is also observed under optical excitation in Fig. 1a. The band at 700 nm in Figs. 3a,b appears only after high dose gamma irradiation which suggests that it is related to a defect created upon exposure to a high dose. Tm does not show any emission in Fig. 3b, and apparently it does not play a role as recombination centre. Tm also does not

create new TL-glow peaks. This is consistent with the VRBE diagram that shows the $Tm^{3+}$ ground state inside the valence band making it unable to trap holes, and the $Tm^{2+}$ is too close to the CB to form a stable electron trap at RT.

According to the VRBE diagram the 4f ground state level of $Ce^{3+}$ is located 3.9 eV above the top of the valence band, and then $Ce^{3+}$ provides a 3.9 eV deep trap for the holes created during irradiation. In the sample doped only with $Ce^{3+}$, exclusively $Ce^{3+}$ emission is present, see Fig. 3c. The glow peak 5 dominates and peaks 1+2 and 6 have low intensity. Fig. 3d for the sample doped with Ce(0.1%) and Tm (0.1%) shows that the presence of Tm reduces the peaks 1+2 and 6 (seen also in Fig. 2d). Additionally, TY increases by 30% upon co-doping with Tm. The exact role of Tm is not yet clear.

The influence of the synthesis atmosphere on storage capacity of $LiLuSiO_4$:Ce,Tm was investigated and vacuum treatment is the best giving TY = 215 compared to air treatment with TY = 4 or $H_2N_2$ treatment with TY = 107 as shown in Fig. 4a. The lower TL intensity of the $H_2N_2$ treated samples as compared to the vacuum treated samples is possibly related with the greyish body color and the additional glow peak 6. The coloration will re-absorb $Ce^{3+}$ emission lowering the amount of light detected during TL. Fig. 5a demonstrates that 475 nm (2.61 eV) blue LED light charges trap 6. It may suggest that 2.61 eV photons excite electrons from so called-thermally disconnected traps (TD) to the shallower traps. TD is defined as a trap which is populated during irradiation but it is not emptied during heating because it is too deep [10, 11] but can be emptied by photon stimulation. The increased temperature during a blue LED excitation (Fig. 5b) allows for further transport of charges to even shallower traps 4 and 5 (Fig. 7b). The overall efficiency of blue-LED-transferred thermoluminescence increases with increasing stimulation temperature.

The increase of the TL intensity for samples prepared in reducing conditions can be assigned to both, increase of the concentration of $Ce^{3+}$ (reduced samples) compared to $Ce^{4+}$ (oxidized samples) and increase of the concentration of oxygen vacancies held responsible for the glow peak 5. It is difficult to specifically disentangle the influence of both effects. However, the higher trap concentration is thought to be a major effect. The presence of a high concentration of $Ce^{4+}$ should lead to a strong brownish coloration of the sample due to the VB to $Ce^{4+}$ charge transfer which is not observed, even for the highest studied concentration of Ce (1%). The fading rate curves presented in Fig. 4b show that the air-

heated-sample exhibit the fastest fading. It is related to the fact, that this sample has a higher population of low temperature traps (~60 $^{o}$C) compared to the higher temperature ones (Fig. 2a). At RT stored electrons have enough thermal energy to escape the shallow trap. The trapped charges in samples heated in reducing conditions are much more stable than in samples heated in air due to the dominance of the high temperature glow peak 5. Among these samples the one heated twice in $H_2N_2$ shows the best stability due to the presence of an additional high temperature shoulder of the peak 5 (in Figs. 3a,b present as a separate glow peak 6).

Fig. 6a shows that the Ce, Tm concentration does not influence significantly either the intensity nor the shape of the glow peak measured after high energy irradiation. However, increasing the concentration of the dopants does lead to a faster fading rate as demonstrated in Fig. 6b. It is partly due to a slight shift of the TL-glow towards lower temperature. Most likely it is due to localized transitions of trapped carriers to neighbouring recombination centres. The probability of such transitions is increased by a shorter trap-to-centre distance caused by concentration increase.

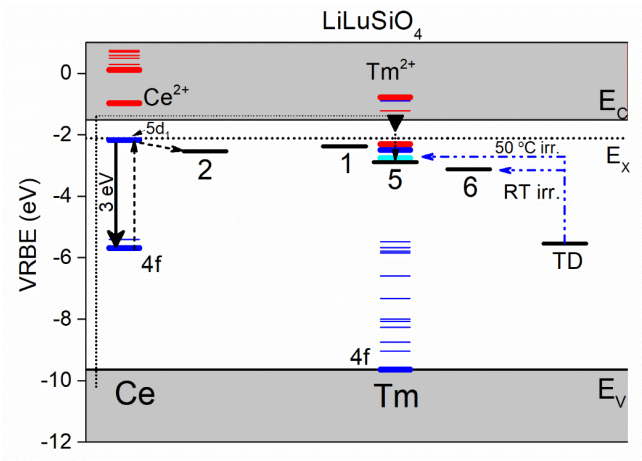


**Figure 9**. The mechanism of the charge carrier transfer during irradiation and readout in $LiLuSiO_4$: Ce, Tm. Levels in red color pertain to divalent and in blue to trivalent Ce or Tm. Traps described in the main text are numbers 1, 2, 5 and 6; $E_V$= energy at the top of the valence band, $E_C$= energy at the bottom of the conduction band, $E_X$= exciton energy, TD= thermally disconnected trap.

Thermoluminescence excitation spectra of glow peak 1 and 3 in Figs. 7a,c,e where Ce and Tm concentration increases from 0.1 to 0.2 to 0.5% are very similar indicating a trap filling mechanism independent on doping concentration. The spectra are dominated by a broad band with a maximum around 280 nm (4.43 eV). It is attributed to the absorption of an electron from the ground state of $Ce^{3+}$ to the conduction band or absorption bands related to the defects other than $Ce^{3+}$. TLES of glow peak 2 is dominated by the band with maximum at around 360 nm which overlaps with the first 4f-$5d_1$ excitation band of $Ce^{3+}$ (Fig. 7b). The 4f-$5d_{2,3}$ (seen in PLES of $Ce^{3+}$) are absent in TLES of peak 2.

All above results allow us to propose the mechanism of charge carrier transfer during charging and readout in $LiLuSiO_4$:Ce,Tm storage phosphor (Fig. 9) . The location of the $Ce^{3+/2+}$ and $Tm^{3+/2+}$ 4f and 5d level energies are extracted from the vacuum referred energy level scheme pertaining to Ln in $LiLuSiO_4$. The trap depth of glow peak 5 is from the heating rate plot and the locations of the levels of peaks 1, 2 and 6 are derived from the one of peak 5.

Trap levels indicated as 1, 2, 5 and 6 correspond to the glow peaks observed in TL (Figs. 3, 4, 7). The traps with glow peaks 3 and 4 are not indicated due to the minor intensity. TD denotes so-called thermally disconnected trap. The trap with a glow peak 6 is observed only after very high dose γ-irradiation in vacuum treated samples (Fig. 3) and as a shoulder of peak 5 in samples repeatedly heated in $H_2$-$N_2$ atmosphere (Fig.4a, dotted line). During high energy irradiation with beta's (dotted black arrow) electrons are raised from the valence band to the conduction band and captured by all traps but mainly 5. The holes left in valence band are captured by $Ce^{3+}$ which turns into $Ce^{4+}$. During optical excitation (dashed black line) electrons are raised form the 4f ground state of $Ce^{3+}$ to $5d_1$ ($\lambda_{exc.}$ = 360 nm, 3.4 eV). According to the Ln energy level scheme for $LiLuSiO_4$, the $5d_1$ state is placed 0.6 eV below the bottom of the conduction band. This distance is too large for efficient thermal ionization of an electron from the $5d_1$ level to the conduction band at room temperature. The electron is assumed to be transferred from the $5d_1$ excited state of $Ce^{3+}$ to a neighboring defect responsible for the glow peak 2. The intensity of this glow peak increases with concentration (Figs. 7b, d, f) because the probability of the localized transfer strongly increases for shorter $Ce^{3+}$-trap distances. The trap which are located at larger distance from $Ce^{3+}$ can be filled only via transfer of electrons from the conduction band.

Higher energy optical excitation ($\lambda_{exc.}$ = 280 nm, 4.4 eV) raises electrons from 4f ground state of $Ce^{3+}$ to the conduction band and from there they are captured by all traps. It is not excluded that $\lambda_{exc.}$ = 280 nm raises electrons from an impurity state different than $Ce^{3+}$ to the conduction band. For the sake of clarity this possibility is not included in Fig. 9 . During optical excitation an electron is taken from the 4f ground state of $Ce^{3+}$ and leaves $Ce^{4+}$. Blue arrows (dash dot dot) show the photo-transfer (blue LED, $\lambda_{stim.}$ = 475 nm, 2.6 eV) of electrons from TD to shallower trap 6 at 25 $^{o}$C (Fig. 5a) and traps 4, 5 and 6 at 50 $^{o}$C (Fig. 5b). Upon heating electrons freed from all available traps recombine with holes captured by $Ce^{3+}$ leaving $Ce^{3+}$ in an excited state which upon return emits a photon with 410 nm, 3.0 eV.

## 5. Conclusions

In $LiLuSiO_4$:Ce,Tm, $Ce^{3+}$ is a hole trapping centre. Oxygen vacancies are the most probable electron trapping centres. Neither Tm nor Ca, Hf, Al, Ge play a role of additional electron traps. Tm-doping has a clear positive effect on storage properties but its exact role is not yet clear. There are electron traps which are distant and close to $Ce^{4+}$-recombination centre. The close traps (glow peak 2) are filled via localized transfer of an electron from $5d_1$ of $Ce^{3+}$. The higher the Ce, Tm concentration, the higher the population of this trap. Distant traps (mainly glow peak 5) are populated via transfer of an electron from the conduction band. The presence of the low temperature glow peak leads to fading, thus it deteriorates the overall storage capability. The large separation between defects in storage phosphors provides the best stability of charges.

## References

[1] Dobrowolska, A., Bos, A.J.J., Dorenbos, P., 2019. High Charge Carrier Storage Capacity in Lithium Lutetium Silicate Doped with Cerium and Thulium. Phys. Status Solidi RRL. 13, 1800502. https://doi.org/10.1002/pssr.201800502

[2] Leblans, P., Vandenbroucke, D., Willems P., 2011. Storage Phosphors for Medical Imaging. Materials 4(6), 1034. https://doi: 10.3390/ma4061034

[3] Nakayama, N., Sakamoto, M., 1992. Microstructures and Electrical Properties for LiXSiO4 (X=Al, Y, La, Nd, Sm, Gd, Dy, Ho, Er, Yb). J. Ceram. Soc. Jpn. 100(6), 867.

[4] Bos, A. J.J., 2007. Theory of Thermoluminescence, Radiat. Meas. 41, S45–S56. https://doi.org/10.1016/j.radmeas.2007.01.003

[5] Sidorenko, A. V., Bos, A. J. J., Dorenbos, P., van Eijk, C.W.E., Kahn-Harari, A., Rodnyi, P.A., Viana, B., 2005. Storage effect in LiRESiO4: Ce3+, Sm3+, RE= Y, Lu phosphor. Nucl. Instrum. and Meth. Phys, Res. A. 537, 81. https://doi.org/10.1016/j.nima.2004.07.239

[6] Sidorenko, A.V., Dorenbos, P., Bos, A.J.J., van Eijk C.W.E., Rodnyi, P.A., 2006. Lanthanide level location and charge carrier trapping in LiLnSiO4:Ce3+,Sm3+, Ln = Y or Lu. J. Phys.: Condens. Matter. 18, 4503. https://doi.org/10.1088/0953-8984/18/19/006

[7] Dorenbos, P., 2017. Charge transfer bands in optical materials and related defect level location. Opt. Mater. 69, 2. https://doi.org/10.1016/j.optmat.2017.03.061

[8] Dorenbos, P., 2013. Ce3+ 5d-centroid shift and vacuum referred 4f-electron binding energies of all lanthanide impurities in 150 different compounds. J. Lumin. 135, 93. https://doi.org/10.1016/j.jlumin.2012.09.034

[9] Dhar, A., Dewerd, L.A., Stoebe T. G., 1973. Effects of annealing and cooling processes on thermoluminescence of LiF (TLD100). Health Physics. 25, 351-441.

[10] Ortega, F., Marcazzó, J., Molina, P., Santiago, M., Lester, M., Henniger, J., Caselli, E., 2013. Analysis of the main dosimetric peak of Al2O3:C compounds with a model of interacting traps. Appl. Radiat. Isotopes. 78, 33. https://doi.org/10.1016/j.apradiso.2013.02.023

[11] McKeever, S. W. S., 1994. Thermoluminescence of solids, Cambridge University Press.